Editors' Suggestion

Strong Zero Modes in Integrable Quantum Circuits

Eric Vernier,[1] Hsiu-Chung Yeh,[2] Lorenzo Piroli,[3] and Aditi Mitra[2]

[1]*Laboratoire de Probabilités, Statistique et Modélisation CNRS—Université Paris Cité—Sorbonne Université. Paris, France*

[2]*Center for Quantum Phenomena, Department of Physics, New York University, 726 Broadway, New York, New York 10003, USA*

[3]*Dipartimento di Fisica e Astronomia, Università di Bologna and INFN, Sezione di Bologna, via Irnerio 46, I-40126 Bologna, Italy*

(Received 20 February 2024; revised 7 May 2024; accepted 28 June 2024; published 2 August 2024)

It is a classic result that certain interacting integrable spin chains host robust edge modes known as strong zero modes (SZMs). In this Letter, we extend this result to the Floquet setting of local quantum circuits, focusing on a prototypical model providing an integrable Trotterization for the evolution of the XXZ Heisenberg spin chain. By exploiting the algebraic structures of integrability, we show that an exact SZM operator can be constructed for these integrable quantum circuits in certain regions of parameter space. Our construction, which recovers a well-known result by Paul Fendley in the continuous-time limit, relies on a set of commuting transfer matrices known from integrability, and allows us to easily prove important properties of the SZM, including normalizabilty. Our approach is different from previous methods and could be of independent interest even in the Hamiltonian setting. Our predictions, which are corroborated by numerical simulations of infinite-temperature autocorrelation functions, are potentially interesting for implementations of the XXZ quantum circuit on available quantum platforms.

DOI: 10.1103/PhysRevLett.133.050606

Introduction—It is well-known that certain one-dimensional quantum spin chains host robust edge modes known as strong zero modes (SZMs) [1–4]. A SZM is an operator Ψ localized at the edges of the system, commuting with the Hamiltonian H in the thermodynamic limit, and anticommuting with one of its discrete symmetries $\mathcal{D}$. The existence of such a SZM implies that the entire spectrum of the Hamiltonian comes in degenerate pairs, corresponding to eigenstates living in different symmetry sectors.

In the past decade, SZMs have attracted significant attention [5–14] because their presence leads to remarkable spectral and dynamical features, such as nonergodic effects and arbitrarily long coherence times for the edge spins, with potential applications to quantum-information storage and processing [15].

A canonical example of SZM is found in the noninteracting transverse-field Ising model in the ordered phase, with free open boundary conditions [1]. Although the edge modes become typically unstable at high temperatures when interactions are turned on (while staying stable at zero temperature [16,17]), their lifetime can be nonperturbative in the interaction strength [5,6,18–21], yielding long-lived quasistable modes referred to as almost strong zero modes [5]. In fact, a classic result by Paul Fendley [4] shows that *exact* strong zero modes can survive the presence of *integrable* interactions, as seen in the XYZ spin chain, a prototypical model of an interacting, integrable system [22].

The notion of SZMs can be extended to Floquet-driven systems [23–26]. In this case the structure of edge modes is known to be richer than in the Hamiltonian setting [27–32], with the possibility of hosting so-called strong π modes (SπMs) [9,25]. Denoting by U the Floquet unitary over one drive cycle, the SZM and the SπM satisfy $\{\Psi_{0,\pi}, \mathcal{D}\} = 0$ and $\Psi_{0,\pi}^2 = O(1)$, while $[\Psi_0, U] \simeq 0$, $\{\Psi_\pi, U\} \simeq 0$, respectively. Both operators give rise to a splitting of the spectrum into pairs of eigenstates with opposite symmetry [33–35].

Edge modes in interacting Floquet systems have been studied in different settings, such as in the high-frequency limit [36] or in the Floquet many-body localization context [29,37–40]. For nondisordered systems and away from the high-frequency limit, numerical evidence along with analytic estimates support that edge modes survive the presence of interactions over long timescales [9,41,42], but a natural question is whether exact SZMs (or SπMs) are possible for interacting integrable Floquet dynamics.

This is the question we tackle in this Letter. We consider a family of Floquet systems where the cycle operator U is written in terms of geometrically local two-spin (or two-qubit) unitaries, called quantum gates, cf. Fig. 1. We focus on circuits providing a Trotterization for the XXZ Heisenberg spin chain [43–45], being both integrable and interacting. These models have recently attracted significant attention [46–50], both because of their rich dynamical features [47,50] and due to the possibility of realizing them on available quantum computers, as already exemplified in recent experimental work [51–53]. Our results show that integrable quantum circuits make it possible to observe exact SZMs in the presence of interactions.

From the technical point of view, we develop a construction rooted in the structures of integrability [22], which

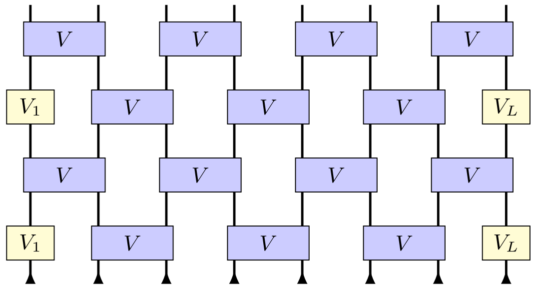

FIG. 1. Pictorial representation of the quantum circuits considered in this Letter. Time runs upward and lower (upper) lines correspond to input (output) degrees of freedom. Each time cycle consists of two time steps where the two-qubit gates couple qubits $(2j, 2j+1)$ and $(2j+1, 2j+2)$, respectively (in the picture, we chose $L = 8$ sites and $t = 2$).

is different from previous approaches [4] and thus of independent interest even in the Hamiltonian setting. In unpublished work [54], Fendley and Verstraete have found, for the XYZ Hamiltonian, a family of commuting matrix-product operators that generate the SZM of [4]. Our construction is different and makes the precise connection with integrability explicit: since it is derived from simple algebraic constraints imposed on the usual transfer matrices of boundary integrability, we expect it to be naturally extended to other integrable Hamiltonians or quantum circuits [55].

The model—We consider a system of $L = 2M$ qubits, i.e., two-level quantum systems spanned by the basis states $|0\rangle, |1\rangle$. The dynamics is discrete, and driven by the unitary operator $U = U_\mathrm{e} U_\mathrm{o}$, where

$$U_\mathrm{e} = V_{12} V_{34} \ldots V_{L-1,L}, \tag{1a}$$

$$U_\mathrm{o} = V_1 V_{23} \ldots V_{L-2,L-1} V_L. \tag{1b}$$

The two-qubit unitary gates are parametrized as [43,44]

$$V = e^{-i\frac{\tau}{4}[\sigma^x \otimes \sigma^x + \sigma^y \otimes \sigma^y + \tilde{\Delta}(\sigma^z \otimes \sigma^z - \mathbb{1})]}, \tag{2}$$

while the matrices V_1 and V_L are single-qubit unitary gates acting on the edge qubits. A pictorial representation of the quantum circuit is displayed in Fig. 1.

Contrary to previous work, we are interested in open boundary conditions. There are different choices for the operators V_1 and V_L that preserve the integrability of the operator U. We focus on the simplest case where the left boundary condition is free, i.e., we set $V_1 = \mathbb{1}$. Usually, SZMs are discussed in the limit of a semi-infinite chain [4], where the choice of the right boundary condition becomes immaterial. Here, however, we construct an exact zero mode for a finite size system by fine-tuning the right boundary condition. Anticipating our result, we will show that an exact SZM exists for finite system sizes when

$$V_L = \mathcal{N}^{-1} \begin{pmatrix} \sinh\left(\sigma\eta + i\frac{x}{2}\right) & 0 \\ 0 & \sinh\left(\sigma\eta - i\frac{x}{2}\right) \end{pmatrix}, \tag{3}$$

where $\sigma = \pm 1$ is fixed, $\mathcal{N} = \sinh[\eta + i(x/2)]\sinh[\eta - i(x/2)]$ is a normalization factor, while η and x are related to $\tilde{\Delta}$, and τ in (2) by

$$\cosh\eta = \frac{\sin\frac{\tilde{\Delta}\tau}{2}}{\sin\frac{\tau}{2}}, \qquad \sin x = -\sinh\eta \tan\frac{\tau}{2}. \tag{4}$$

We consider $\eta, x \in \mathbb{R}$, corresponding to the "gapped phase" of the model [44]. The name refers to the fact that the structure of the conserved charges is the same as the gapped XXZ Hamiltonian [50], as well as the classification of Floquet eigenstates in terms of "Bethe strings" [48].

Similar to the Hamiltonian case [4], we will find that SZMs exist in the "gapped phase" of the quantum-circuit model [44,50], to which the rest of this Letter is restricted. The continuous-time limit can be recovered by $x \to 0$, that is $\tau \to 0$, yielding

$$H = \sum_{i=1}^{L-1} [\sigma_i^x \sigma_{i+1}^x + \sigma_i^y \sigma_{i+1}^y + \cosh\eta(\sigma_i^z \sigma_{i+1}^z - 1)] + h_1 \sigma_1^z + h_L \sigma_L^z, \tag{5}$$

where $h_1 = 0$, $h_L = \sigma\cosh\eta$. (5) is the XXZ Hamiltonian in the gapped phase, with boundary fields h_1, h_L.

Commuting transfer matrices—In order to construct the SZMs, we follow an original strategy, making use of algebraic tools from integrability. The idea is to embed the SZMs in a family of commuting transfer matrices with open boundary conditions [56–59], which are written as a trace over some auxiliary qubit "0",

$$T(u) = \mathrm{tr}_0\left(K_0^+(u) T_0(u) K_0^-(u) \hat{T}_0(u)\right), \tag{6}$$

$$T_0(u) = R_{01}(u+\xi_1) \ldots R_{0L}(u+\xi_L), \tag{7}$$

$$\hat{T}_0(u) = R_{L0}(u-\xi_L) \ldots R_{10}(u-\xi_1), \tag{8}$$

where the operators $R_{ij}(u)$ acting on the qubits i and j, are called R matrices. In the computational basis $\{|0,0\rangle, |0,1\rangle, |1,0\rangle, |1,1\rangle\}$ they take the form

$$R(u) = \begin{pmatrix} 1 & 0 & 0 & 0 \\ 0 & \frac{\sinh(u)}{\sinh(u+\eta)} & \frac{\sinh\eta}{\sinh(u+\eta)} & 0 \\ 0 & \frac{\sinh\eta}{\sinh(u+\eta)} & \frac{\sinh(u)}{\sinh(u+\eta)} & 0 \\ 0 & 0 & 0 & 1 \end{pmatrix}, \tag{9}$$

where u is the so-called spectral parameter, which can be thought of as controlling the space and time anisotropy of the interaction and allows to tune from a continuous-time Hamiltonian dynamics to a circuitlike geometry. It is

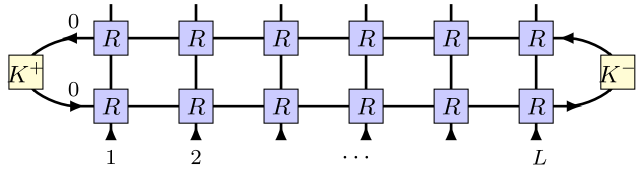

FIG. 2. The transfer matrix $T(u)$ of (6). The qubits $i = 1\ldots L$ correspond to the vertical lines from left to right, while the horizontal lines are associated with an auxiliary two-dimensional Hilbert space. The blue boxes are four-leg tensors acting as (9) with argument $u + \xi_i$ (top row) or $u - \xi_i$ (bottom row), while the yellow boxes are matrices acting as (10) on the auxiliary space. Choosing the parameters as in (12), the transfer matrix coincides with the evolution operator U for the quantum circuit.

convenient to represent the transfer matrix using common tensor-network conventions [60], cf. Fig. 2. In this notation, each operator is viewed as a multi-index tensor and represented by a box with multiple legs. One also makes a distinction between physical indices, corresponding to the physical degrees of freedom, and auxiliary ones. For example, the R matrices are four-tensors with four legs, two physical and two auxiliary ones (one pair for each of the local spaces it acts on). Finally, joined legs in Fig. 2 correspond to pairs of sums over indices [60].

The parameters ξ_j play the role of spatial inhomogeneities, while matrices $K^{\pm}(u)$ are known as reflection matrices. We will restrict to the case where they are diagonal, taking the form

$$K^{\pm}(u) = K(u + \eta/2 \pm \eta/2, \xi_{\pm}), \tag{10}$$

$$K(u, \xi) = \begin{pmatrix} \sinh(\xi + u) & 0 \\ 0 & \sinh(\xi - u) \end{pmatrix}, \tag{11}$$

where the parameters $\xi_{\pm}$ will be specified below. This choice of the R and K matrices ensures that they satisfy the Yang-Baxter [61] and the reflection (or boundary Yang-Baxter) equations [56], respectively. As a result, transfer matrices associated with different spectral parameters u commute, $[T(u), T(v)] = 0$.

In order to make connection with the circuit described above, we need to specify the value of the parameters $\xi_{\pm}$ and ξ_j. More explicitly, we set

$$\xi_+ = i\frac{\pi}{2}, \qquad \xi_- = \sigma\eta, \qquad \xi_j = (-1)^j \frac{ix}{2}. \tag{12}$$

It is a simple exercise [62] to see that the operator $T(u)$ evaluated at a special value of the spectral parameter $u = ix/2$ reduces, up to a proportionality factor, to the brickwork circuit generator U (see Ref. [43] for an analogous construction in the periodic case).

Note that the continuous-time limit corresponds to $x = 0$. In this case, the transfer matrix $T(0)$ is proportional to the identity, but the XXZ Hamiltonian (5) can be generated by the logarithmic derivative [22,62]

$$T(0)^{-1}T'(0) = \frac{1}{\sinh\eta}\left(H - \frac{1}{\cosh\eta}\mathbb{1}\right). \tag{13}$$

The zero mode—Both in the circuit and Hamiltonian cases, the generator of the dynamics (that is, respectively, U or H), commutes with the continuous family of transfer matrices $T(u)$. Indeed, the latter generate the set of homogeneous local conserved operators, or charges, which are the hallmark of integrability [22].

Note, however, that $T(u)$ are not themselves local operators: in order to generate the local charges one needs to take logarithmic derivatives of them. In the continuous-time limit, for instance, the first-order one yields the Hamiltonian, cf. (13), while additional charges are obtained by higher-order derivatives. Crucially, such derivatives must be taken at the spectral parameter $u = 0$, where (SI.5) holds. Indeed, it is this regularity condition which ensures locality [22].

Our construction relies on a different mechanism, and as a consequence, yields a distinct family of conserved quantities. Contrary to the standard charges, the latter are (quasi)localized at the left boundary of the system and, as we will show, feature the SZM. The idea, which is one of the main technical contributions of our Letter, is to take the derivatives around the point $u = i\pi/2$, instead of $u = 0$. In this case, the regularity condition (SI.5) is replaced by

$$R_{j0}\left(\frac{i\pi}{2} \pm \frac{ix}{2}\right)\sigma_0^z R_{0j}\left(\frac{i\pi}{2} \mp \frac{ix}{2}\right) = \sigma_0^z, \tag{14}$$

which we write pictorially as

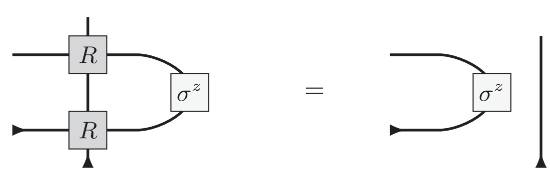

(15)

Exploiting the form of the boundary matrices $K^{\pm}$, (14) allows one to show that the derivatives of the transfer matrix at $u = i\pi/2$ are localized near the left boundary. As we discuss in the Supplemental Material (SM) [62], the underlying mechanism is simple and can be illustrated graphically by repeated use of (15). Therefore, it is natural to conjecture that the SZM can be defined as the derivative

$$\Psi(x) = \frac{i\mathcal{N}(x)}{2\sinh^2\eta} T'(i\pi/2), \tag{16}$$

where $\mathcal{N}(x) = \cosh[\eta + (ix/2)) \cosh(\eta - (ix/2)]/\cosh^2\eta$ is a normalization constant introduced for later convenience. In the rest of this Letter we will show the validity of this conjecture.

Before proceeding, it is important to note that the right-hand side of (16) can be made more explicit. The derivation is technically involved and is carried out in the SM [62], while here we only report the final result. Introducing the auxiliary functions $t_a(x) = (-1)^a \tanh\eta \tanh(ix/2)$, $\Delta(x) = \{\cosh[\eta + (ix/2)] \cosh[\eta - (ix/2)]/\cos^2(x/2)\}^{1/2}$ and

$$\widetilde{\sigma_b^z} := \begin{cases} \sigma_b^z & \text{if } b \leq L \\ \mathcal{N}(x)\sigma & \text{if } b = L+1 \end{cases} \tag{17}$$

we can rewrite

$$\Psi(x) = \sum_{S=0}^{\lfloor L/2 \rfloor} \sum_{\{a\}_{2S},b} \frac{1}{\Delta(x)^{2b-2}} \left(\prod_{s=1}^{S} \langle a_{2s-1} a_{2s} \rangle \right) \widetilde{\sigma_b^z} + \sum_{S=1}^{\lfloor L/2 \rfloor} \sum_{\{a\}_{2S}} \frac{1}{\Delta(x)^{2a_{2S}}} \left(\prod_{s=1}^{S-1} \langle a_{2s-1} a_{2s} \rangle \right) \overline{\langle a_{2S-1} a_{2S} \rangle}, \tag{18}$$

where $\langle aa' \rangle = -2\{\sinh^2\eta/[\cos^2(x/2)]\} \langle aa' \rangle_+$, and $\overline{\langle aa' \rangle} = -t_{a'}(x)\Delta(x)^2 \langle aa' \rangle_-$, with the brackets $\langle aa' \rangle_\pm$ defined as

$$\langle aa' \rangle_\pm = (\cosh\eta)^{a'-a} \left[\sigma_a^+ \left(\prod_{a<k<a'} (1 + t_k(x)\sigma_k^z) \right) \sigma_{a'}^- \pm \sigma_a^- \left(\prod_{a<k<a'} (1 - t_k(x)\sigma_k^z) \right) \sigma_{a'}^+ \right]. \tag{19}$$

In (18) the outer sum is over all sets of integers $0 < a_1 < \ldots < a_{2S} < b \leq L+1$, while the inner sum is over all sets of integers $0 < a_1 < \ldots < a_{2S} \leq L$.

Equation (18) is the first main result of our Letter. In the following, we will claim that this operator is a genuine SZM for the quantum-circuit dynamics. Note that, in the limit $x \to 0$, we recover the exact expression obtained by Paul Fendley in Ref. [4] using a different derivation.

Properties of the SZM—It follows from our previous discussion that $\Psi(x)$ commutes with the Floquet operator U. In order to show that it is a genuine SZM, we need to verify the following properties [4]: (i) it anticommutes with the $\mathbb{Z}_2$ symmetry $X = \prod_j \sigma_j^x$; (ii) it squares to 1, i.e., $\Psi^2(x) \propto \mathbb{1}$, in the thermodynamic limit; (iii) it is quasilocalized at the boundary of the chain.

First, it is easy to see that, similar to the Hamiltonian case [4], anticommutation with the $\mathbb{Z}_2$ symmetry holds in the thermodynamic limit (as for finite L it flips the value of the boundary spin σ). Conversely, properties (ii) and (iii) require a more technical analysis. This is reported in the SM [62], where we prove that they are satisfied. We stress that the transfer matrix representation makes our derivations relatively simple [63–65]. In addition, having expressed the SZM in terms of standard objects from integrability, we expect that our constructions and derivations may be readily extended to more general spin chains and quantum circuits [62].

Physical consequences of the SZM—As we have mentioned, the existence of SZMs has important consequences for the system dynamics. In particular, it is expected that edge dynamical correlation functions do not decay in the large-time limit. We provide numerical evidence that this is indeed the case for the XXZ integrable quantum circuit.

We consider the infinite-temperature dynamical correlation function

$$C(t) = \frac{\mathrm{Tr}[\sigma_1^z(t)\sigma_1^z(0)]}{2^L}, \tag{20}$$

where t is discrete time. Heuristically, consider $\sigma_1^z = \sum_j c_j O_j$, where O_j is an orthogonal operator basis, satisfying $\mathrm{Tr}[O_j^\dagger O_k]/2^L = \delta_{j,k}$. Choosing $O_1 \propto \Psi(x)$, one has $C(t) = |c_1|^2 + f(t)$, where $f(t) = \sum_{j,k>1} c_j c_k \mathrm{Tr}[(U^\dagger)^t O_j U^t O_k]$. Denoting

$$\bar{f} = \lim_{N\to\infty} \frac{1}{N} \sum_{t=1}^{N} f(t), \tag{21}$$

and assuming that $\bar{f}$ vanishes in the thermodynamic limit, we obtain the prediction

$$\lim_{L\to\infty} \bar{C} = \frac{\mathrm{Tr}[\Psi(x)\sigma_1^z]}{2^{L/2}\sqrt{\mathrm{Tr}[\Psi(x)^2]}} = \frac{\sinh^2\eta}{c^{(-)}(\eta)c^{(+)}(\eta)}, \tag{22}$$

with $c^{(\pm)}(\eta) = \cosh(\eta \pm ix/2)$, and where the second equality follows from (18), cf. [62].

The assumption that $\bar{f}$ vanishes in the thermodynamic limit is reasonable provided that there are not any additional edge modes independent of $\Psi(x)$. Other local conserved quantities may have nonzero overlap with σ_1^z, but the latter are expected to vanish in the thermodynamic limit. For instance, defining the (normalized) local charge $S_z = (1/\sqrt{L}) \sum_j \sigma_j^z$, so that $\mathrm{Tr}[S_z^2]/2^L = 1$, we have $\mathrm{Tr}[S_z\sigma_1^z] = 1/\sqrt{L}$.

We have performed extensive numerical calculations to test the decay of $C(t)$ and the validity of our prediction (22).

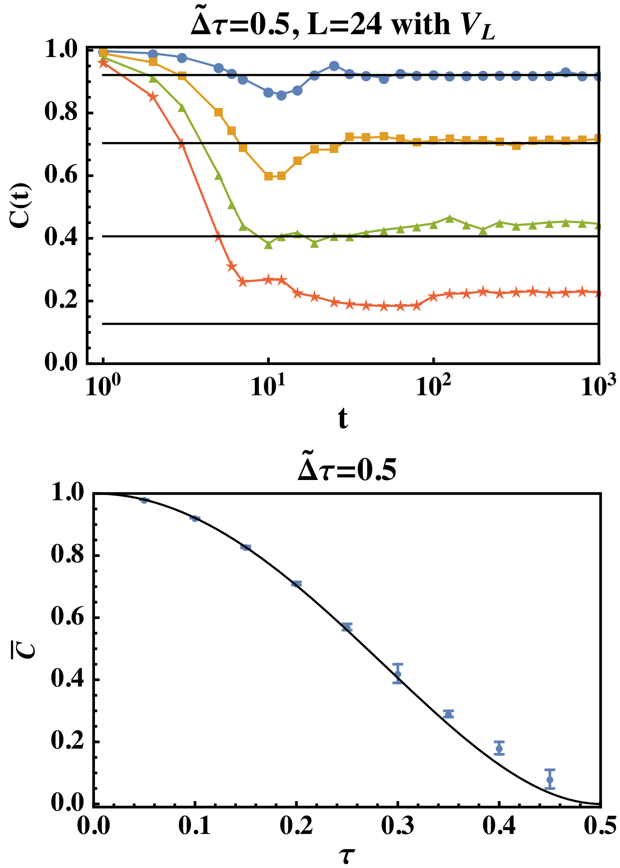

FIG. 3. Numerical results for the autocorrelation functions. Top: $C(t)$ as a function of time, for different τ values $\tau = 0.1, 0.2, 0.3, 0.4$ (increasing from top to bottom) with fixed $\tilde{\Delta}\tau = 0.5$. Bottom: averaged value $\bar{C}$ in the thermodynamic limit $L \to \infty$ with fixed $\tilde{\Delta}\tau = 0.5$. Solid lines correspond to the analytic result (22), while dots are obtained via the numerical fitting procedure explained in the main text. The plot also displays the corresponding estimated errors.

We used an efficient numerical approach based on quantum typicality [66,67] to simulate $C(t)$ for system sizes and times up to $L = 24$ and $t = 10^3$, respectively. For small sizes we have checked the validity of our approach against exact numerical computations.

After a transient time, we found that $C(t)$ approaches a plateau, with small persisting fluctuations. For each L, we have estimated the late time average $\bar{C}_L$ and found, roughly, $\bar{C}_L \sim a + b/L$ for large L. By means of a numerical fit, we have finally estimated the large-L limit and repeated this whole procedure for different values of the circuit parameters, $\tilde{\Delta}$ and τ. An example of our results is reported in Fig. 3. Our data show very clearly that $\bar{C}$ does not vanish in the thermodynamic limit, and we obtained quantitative agreement with the prediction (22). We have found that the discrepancy between the analytic and numerical results increases as we move closer to the transition from the "gapless" to the "gapped" phases [50], and interpret these discrepancies as arising from finite-size effects.

While exact SZMs are expected to be a feature of integrable systems, it was observed in the Hamiltonian case that approximately conserved SZMs persist in the absence of integrability, resulting in exponentially long-lived correlations [5]. We check here that this feature extends to the Floquet setting: studying the quantity $C(t)$ in the presence of integrability-breaking disorder, we indeed observe the presence of long-lived correlations [62].

Outlook—We have constructed an exact SZM operator for a class of integrable, interacting Floquet dynamics consisting of local quantum circuits. We showed by numerical computations that the presence of the SZM can be detected by probing the boundary dynamical correlation functions, making our results potentially relevant for present-day implementation of integrable quantum circuits [51–53]. Our Letter opens several directions for future studies. First, it would be very interesting to investigate the presence of SπMs in the context of integrable quantum circuits, and to understand whether they can be constructed using techniques similar to those presented here. Second, our approach is based on standard algebraic Bethe ansatz techniques that we believe could be extended to more general models. It would be interesting, for instance, to study local quantum circuits such as those constructed in [68], or which are obtained by Trotterizing $SU(N)$-invariant spin chains and their deformations. Third, we could use our construction to illuminate the effect of SZMs or SπMs on the Bethe ansatz spectrum of the considered models [69–71]. We leave these questions for future work.

Acknowledgments—E. V. thanks Paul Fendley for discussions and for sharing some unpublished results. L. P. and A. M. acknowledge hospitality from the Simons Center for Geometry and Physics, Stony Brook University, during the program "Fluctuations, Entanglements, and Chaos: Exact Results," where this research was initiated. H. Y. acknowledges support of the NYU IT High Performance Computing resources, services, and staff expertise. This work was supported by the US Department of Energy, Office of Science, Basic Energy Sciences, under Award No. DE-SC0010821 (H. Y., A. M.).

[1] A. Y. Kitaev, Unpaired Majorana fermions in quantum wires, Phys. Usp. **44**, 131 (2001).
[2] P. Fendley, Parafermionic edge zero modes in Zn-invariant spin chains, J. Stat. Mech. (2012) P11020.
[3] A. S. Jermyn, R. S. K. Mong, J. Alicea, and P. Fendley, Stability of zero modes in parafermion chains, Phys. Rev. B **90**, 165106 (2014).
[4] P. Fendley, Strong zero modes and eigenstate phase transitions in the XYZ/interacting Majorana chain, J. Phys. A **49**, 30LT01 (2016).

[5] J. Kemp, N. Y. Yao, C. R. Laumann, and P. Fendley, Long coherence times for edge spins, J. Stat. Mech. (2017) 063105.
[6] D. V. Else, P. Fendley, J. Kemp, and C. Nayak, Prethermal strong zero modes and topological qubits, Phys. Rev. X **7**, 041062 (2017).
[7] L. M. Vasiloiu, F. Carollo, and J. P. Garrahan, Enhancing correlation times for edge spins through dissipation, Phys. Rev. B **98**, 094308 (2018).
[8] L. M. Vasiloiu, F. Carollo, M. Marcuzzi, and J. P. Garrahan, Strong zero modes in a class of generalized Ising spin ladders with plaquette interactions, Phys. Rev. B **100**, 024309 (2019).
[9] D. J. Yates, F. H. L. Essler, and A. Mitra, Almost strong $(0,\pi)$ edge modes in clean interacting one-dimensional floquet systems, Phys. Rev. B **99**, 205419 (2019).
[10] D. J. Yates and A. Mitra, Strong and almost strong modes of floquet spin chains in Krylov subspaces, Phys. Rev. B **104**, 195121 (2021).
[11] N. Laflorencie, Universal signatures of Majorana zero modes in critical kitaev chains, arXiv:2311.07571.
[12] N. Chepiga and N. Laflorencie, Topological and quantum critical properties of the interacting Majorana chain model, SciPost Phys. **14**, 152 (2023).
[13] N. Laflorencie, G. Lemarié, and N. Macé, Topological order in random interacting Ising-Majorana chains stabilized by many-body localization, Phys. Rev. Res. **4**, L032016 (2022).
[14] H.-C. Yeh, G. Cardoso, L. Korneev, D. Sels, A. G. Abanov, and A. Mitra, Slowly decaying zero mode in a weakly nonintegrable boundary impurity model, Phys. Rev. B **108**, 165143 (2023).
[15] S. D. Sarma, M. Freedman, and C. Nayak, Majorana zero modes and topological quantum computation, npj Quantum Inf. **1**, 1 (2015).
[16] H. Katsura, D. Schuricht, and M. Takahashi, Exact ground states and topological order in interacting Kitaev/Majorana chains, Phys. Rev. B **92**, 115137 (2015).
[17] J.-J. Miao, H.-K. Jin, F.-C. Zhang, and Y. Zhou, Exact solution for the interacting Kitaev chain at the symmetric point, Phys. Rev. Lett. **118**, 267701 (2017).
[18] D. E. Parker, R. Vasseur, and T. Scaffidi, Topologically protected long edge coherence times in symmetry-broken phases, Phys. Rev. Lett. **122**, 240605 (2019).
[19] J. Kemp, N. Y. Yao, and C. R. Laumann, Symmetry-enhanced boundary qubits at infinite temperature, Phys. Rev. Lett. **125**, 200506 (2020).
[20] D. J. Yates, A. G. Abanov, and A. Mitra, Lifetime of almost strong edge-mode operators in one-dimensional, interacting, symmetry protected topological phases, Phys. Rev. Lett. **124**, 206803 (2020).
[21] D. J. Yates, A. G. Abanov, and A. Mitra, Dynamics of almost strong edge modes in spin chains away from integrability, Phys. Rev. B **102**, 195419 (2020).
[22] V. E. Korepin, N. M. Bogoliubov, and A. G. Izergin, *Quantum Inverse Scattering Method and Correlation Functions* (Cambridge University Press, Cambridge, England, 1997), Vol. 3.
[23] L. Jiang, T. Kitagawa, J. Alicea, A. R. Akhmerov, D. Pekker, G. Refael, J. I. Cirac, E. Demler, M. D. Lukin, and P. Zoller, Majorana fermions in equilibrium and in driven cold-atom quantum wires, Phys. Rev. Lett. **106**, 220402 (2011).
[24] V. M. Bastidas, C. Emary, G. Schaller, and T. Brandes, Nonequilibrium quantum phase transitions in the Ising model, Phys. Rev. A **86**, 063627 (2012).
[25] M. Thakurathi, A. A. Patel, D. Sen, and A. Dutta, Floquet generation of Majorana end modes and topological invariants, Phys. Rev. B **88**, 155133 (2013).
[26] G. J. Sreejith, A. Lazarides, and R. Moessner, Parafermion chain with $2\pi/k$ floquet edge modes, Phys. Rev. B **94**, 045127 (2016).
[27] J. K. Asbóth, B. Tarasinski, and P. Delplace, Chiral symmetry and bulk-boundary correspondence in periodically driven one-dimensional systems, Phys. Rev. B **90**, 125143 (2014).
[28] R. Roy and F. Harper, Abelian floquet symmetry-protected topological phases in one dimension, Phys. Rev. B **94**, 125105 (2016).
[29] V. Khemani, A. Lazarides, R. Moessner, and S. L. Sondhi, Phase structure of driven quantum systems, Phys. Rev. Lett. **116**, 250401 (2016).
[30] C. W. von Keyserlingk, V. Khemani, and S. L. Sondhi, Absolute stability and spatiotemporal long-range order in floquet systems, Phys. Rev. B **94**, 085112 (2016).
[31] C. W. von Keyserlingk and S. L. Sondhi, Phase structure of one-dimensional interacting floquet systems. I. Abelian symmetry-protected topological phases, Phys. Rev. B **93**, 245145 (2016).
[32] C. W. von Keyserlingk and S. L. Sondhi, Phase structure of one-dimensional interacting floquet systems. II. Symmetry-broken phases, Phys. Rev. B **93**, 245146 (2016).
[33] K. Sacha and J. Zakrzewski, Time crystals: A review, Rep. Prog. Phys. **81**, 016401 (2017).
[34] V. Khemani, R. Moessner, and S. Sondhi, A brief history of time crystals, arXiv:1910.10745.
[35] D. V. Else, C. Monroe, C. Nayak, and N. Y. Yao, Discrete time crystals, Annu. Rev. Condens. Matter Phys. **11**, 467 (2020).
[36] T. Iadecola, L. H. Santos, and C. Chamon, Stroboscopic symmetry-protected topological phases, Phys. Rev. B **92**, 125107 (2015).
[37] Y. Bahri, R. Vosk, E. Altman, and A. Vishwanath, Localization and topology protected quantum coherence at the edge of hot matter, Nat. Commun. **6**, 7341 (2015).
[38] I.-D. Potirniche, A. C. Potter, M. Schleier-Smith, A. Vishwanath, and N. Y. Yao, Floquet symmetry-protected topological phases in cold-atom systems, Phys. Rev. Lett. **119**, 123601 (2017).
[39] A. Kumar, P. T. Dumitrescu, and A. C. Potter, String order parameters for one-dimensional floquet symmetry protected topological phases, Phys. Rev. B **97**, 224302 (2018).
[40] A. Chandran, V. Khemani, C. R. Laumann, and S. L. Sondhi, Many-body localization and symmetry-protected topological order, Phys. Rev. B **89**, 144201 (2014).
[41] D. Yates, A. Abanov, and A. Mitra, Long-lived period-doubled edge modes of interacting and disorder-free floquet spin chains, Commun. Phys. **5**, 43 (2022).

[42] H.-C. Yeh, A. Rosch, and A. Mitra, Decay rates of almost strong modes in floquet spin chains beyond Fermi's golden rule, Phys. Rev. B **108**, 075112 (2023).

[43] M. Vanicat, L. Zadnik, and T. Prosen, Integrable trotterization: Local conservation laws and boundary driving, Phys. Rev. Lett. **121**, 030606 (2018).

[44] M. Ljubotina, L. Zadnik, and T. Prosen, Ballistic spin transport in a periodically driven integrable quantum system, Phys. Rev. Lett. **122**, 150605 (2019).

[45] M. Medenjak, T. Prosen, and L. Zadnik, Rigorous bounds on dynamical response functions and time-translation symmetry breaking, SciPost Phys. **9**, 003 (2020).

[46] Y. Miao, V. Gritsev, and D. V. Kurlov, Integrable quantum circuits from the star-triangle relation, Quantum **7**, 1160 (2023).

[47] G. Giudice, G. Giudici, M. Sonner, J. Thoenniss, A. Lerose, D. A. Abanin, and L. Piroli, Temporal entanglement, quasiparticles, and the role of interactions, Phys. Rev. Lett. **128**, 220401 (2022).

[48] I. L. Aleiner, Bethe ansatz solutions for certain periodic quantum circuits, Ann. Phys. (Amsterdam) **433**, 168593 (2021).

[49] P. W. Claeys, J. Herzog-Arbeitman, and A. Lamacraft, Correlations and commuting transfer matrices in integrable unitary circuits, SciPost Phys. **12**, 007 (2022).

[50] E. Vernier, B. Bertini, G. Giudici, and L. Piroli, Integrable digital quantum simulation: Generalized Gibbs ensembles and Trotter transitions, Phys. Rev. Lett. **130**, 260401 (2023).

[51] N. Keenan, N. F. Robertson, T. Murphy, S. Zhuk, and J. Goold, Evidence of Kardar-Parisi-Zhang scaling on a digital quantum simulator, npj Quantum Inf. **9**, 72 (2023).

[52] K. Maruyoshi, T. Okuda, J. W. Pedersen, R. Suzuki, M. Yamazaki, and Y. Yoshida, Conserved charges in the quantum simulation of integrable spin chains, J. Phys. A **56**, 165301 (2023).

[53] A. Morvan, T. Andersen, X. Mi, C. Neill, A. Petukhov, K. Kechedzhi, D. Abanin, A. Michailidis, R. Acharya, F. Arute *et al.*, Formation of robust bound states of interacting microwave photons, Nature (London) **612**, 240 (2022).

[54] P. Fendley (Private communication). See also https://www.ocf.berkeley.edu/ehudaltman/workshop2016/wp-content/uploads/2016/06/Fendley.pdf.

[55] E. Vernier (to be published).

[56] E. K. Sklyanin, Boundary conditions for integrable quantum systems, J. Phys. A **21**, 2375 (1988).

[57] N. Kitanine, K. K. Kozlowski, J. M. Maillet, G. Niccoli, N. A. Slavnov, and V. Terras, Correlation functions of the open XXZ chain: I, J. Stat. Mech. (2007) P10009.

[58] N. Kitanine, K. K. Kozlowski, J. M. Maillet, G. Niccoli, N. A. Slavnov, and V. Terras, Correlation functions of the open XXZ chain: II, J. Stat. Mech. (2008) P07010.

[59] L. Piroli, B. Pozsgay, and E. Vernier, From the quantum transfer matrix to the quench action: The Loschmidt echo in XXZ Heisenberg spin chains, J. Stat. Mech. (2017) 023106.

[60] P. Silvi, F. Tschirsich, M. Gerster, J. Jünemann, D. Jaschke, M. Rizzi, and S. Montangero, The Tensor Networks Anthology: Simulation techniques for many-body quantum lattice systems, SciPost Phys. Lect. Notes 8 (2019), 10.21468/SciPostPhysLectNotes.8.

[61] F. Essler, H. Frahm, F. Göhmann, A. Klümper, and V. Korepin, *The One-Dimensional Hubbard Model Cambridge University Press* (Cambridge University Press, Cambridge, England, 2005).

[62] See Supplemental Material at http://link.aps.org/supplemental/10.1103/PhysRevLett.133.050606 for details.

[63] T. Prosen, Open XXZ spin chain: Nonequilibrium steady state and a strict bound on ballistic transport, Phys. Rev. Lett. **106**, 217206 (2011).

[64] R. G. Pereira, V. Pasquier, J. Sirker, and I. Affleck, Exactly conserved quasilocal operators for the XXZ spin chain, J. Stat. Mech. (2014) P09037.

[65] L. Piroli and E. Vernier, Quasi-local conserved charges and spin transport in spin-1 integrable chains, J. Stat. Mech. (2016) 053106.

[66] P. Reimann, Typicality for generalized microcanonical ensembles, Phys. Rev. Lett. **99**, 160404 (2007).

[67] R. Steinigeweg, J. Gemmer, and W. Brenig, Spin and energy currents in integrable and nonintegrable spin-$\frac{1}{2}$ chains: A typicality approach to real-time autocorrelations, Phys. Rev. B **91**, 104404 (2015).

[68] Y. Miao and E. Vernier, Integrable quantum circuits from the star-triangle relation, Quantum **7**, 1160 (2023).

[69] S. Skorik and H. Saleur, Boundary bound states and boundary bootstrap in the Sine-Gordon model with dirichlet boundary conditions, J. Phys. A **28**, 6605 (1995).

[70] A. Kapustin and S. Skorik, Surface excitations and surface energy of the antiferromagnetic XXZ chain by the Bethe ansatz approach, J. Phys. A **29**, 1629 (1996).

[71] S. Grijalva, J. D. Nardis, and V. Terras, Open XXZ chain and boundary modes at zero temperature, SciPost Phys. **7**, 023 (2019).